


SCIENTIFIC ARTICLE

Microstructure Analysis and Reconstruction of a Meniscus

Shuang Zhu, MD, PhD^{1†}, Ge Tong, MD, PhD^{2†}, Jian-ping Xiang, MD, PhD³, Shuai Qiu, MD, PhD³, Zhi Yao, MD, PhD⁴, Xiang Zhou, MD, PhD³, Li-jun Lin, MD, PhD¹ 

¹Department of Joint and Orthopaedics, Zhujiang Hospital, Southern Medical University, ²Department of Medical Ultrasonics, Guangdong Province Key Laboratory of Hepatology Research, The Third Affiliated Hospital of Sun Yat-Sen University and ³Department of Microsurgery, Orthopaedic Trauma and Hand Surgery, the First Affiliated Hospital of Sun Yat-sen University, Guangzhou and ⁴Musculoskeletal Research Laboratory, Department of Orthopaedics and Traumatology, The Chinese University of Hong Kong, Hong Kong, China

Objective: To analyze the characteristics of meniscus microstructure and to reconstruct a microstructure-mimicking 3D model of the meniscus.

Methods: Human and sheep meniscus were collected and prepared for this study. Hematoxylin–eosin staining (HE) and Masson staining were conducted for histological analysis of the meniscus. For submicroscopic structure analysis, the meniscus was first freeze-dried and then scanned by scanning electron microscopy (SEM). The porosity of the meniscus was determined according to SEM images. A micro-MRI was used to scan each meniscus, immersed in distilled water, and a 3D digital model was reconstructed afterwards. A three-dimensional (3D) resin model was printed out based on the digital model. Before high-resolution micro-CT scanning, each meniscus was freeze-dried. Then, micro-scale two-dimensional (2D) CT projection images were obtained. The porosity of the meniscus was calculated according to micro-CT images. With micro-CT, multiple 2D projection images were collected. A 3D digital model based on 2D CT pictures was also reconstructed. The 3D digital model was exported as STL format. A 3D resin model was printed by 3D printer based on the 3D digital model.

Results: As revealed in the HE and Masson images, a meniscus is mostly composed of collagen, with a few cells disseminated between the collagen fiber bundles at the micro-scale. The SEM image clearly shows the path of highly cross-linked collagen fibers, and massive pores exist between the fibers. According to the SEM images, the porosity of the meniscus was 34.1% ($34.1\% \pm 0.032\%$) and the diameters of the collagen fibers were varied. In addition, the cross-linking pattern of the fibers was irregular. The scanning accuracy of micro-MRI was 50 μm . The micro-MRI demonstrated the outline of the meniscus, but the microstructure was obscure. The micro-CT clearly displayed microfibrils in the meniscus with a voxel size of 11.4 μm . The surface layer, lamellar layer, circumferential fibers, and radial fibers could be identified. The mean porosity of the meniscus according to micro-CT images was 33.92% ($33.92\% \pm 0.03\%$). Moreover, a 3D model of the microstructure based on the micro-CT images was built. The microscale fibers could be displayed in the micro-CT image and the reconstructed 3D digital model. In addition, a 3D resin model was printed out based on the 3D digital model.

Conclusion: It is extremely difficult to artificially simulate the microstructure of the meniscus because of the irregularity of the diameter and cross-linking pattern of fibers. The micro-MRI images failed to demonstrate the meniscus

Address for correspondence Li-jun Lin, MD, PhD, Department of Joint and Orthopaedics Surgery, Orthopaedic Center, Zhujiang Hospital, Southern Medical University, 253 Gongye Middle Avenue, Guangzhou, China 510280 Tel: 0086-13822153869; Fax: 0086-020-61643888; Email: gost1@smu.edu.cn; Xiang Zhou, MD, PhD, Department of Microsurgery, Orthopaedic Trauma and Hand Surgery, the First Affiliated Hospital of Sun Yat-sen University, 58 Zhongshan Er Road, Guangzhou, China 510080 Tel: 0086-15913113047; Fax: 0086-020-87332200; Email: 110337622@qq.com

[†]These authors contributed equally to this work.

Disclosure: The authors declare that they have no conflicts of interest. All authors listed meet the authorship criteria according to the latest guidelines of the International Committee of Medical Journal Editors, and all authors are in agreement with the manuscript.

Received 3 June 2020; accepted 22 November 2020

Orthopaedic Surgery 2021;13:306–313 • DOI: 10.1111/os.12899

This is an open access article under the terms of the Creative Commons Attribution-NonCommercial-NoDerivs License, which permits use and distribution in any medium, provided the original work is properly cited, the use is non-commercial and no modifications or adaptations are made.

microstructure. Freeze-drying and micro-CT scanning are effective methods for 3D microstructure reconstruction of the meniscus, which is an important step towards mechanically functional 3D-printed meniscus grafts.

Key words: 3D printing; Freeze-drying; Meniscus; Micro-CT; Micro-MRI

Introduction

As a semilunar fibrocartilaginous tissue between the femoral condyle and tibial plateau, the meniscus assists in load bearing and transmission, joint stabilization, and shock absorption^{1, 2}. It is well known that a torn meniscus and/or surgical removal of the meniscus will result in early articular cartilage damage and, eventually, early osteoarthritis³. Thus, preservation of the function of the meniscus is of great interest for doctors and researchers. Due to limited blood supply of the meniscus, meniscus suture or repair can result in non-healing or secondary surgery. Therefore, meniscal allograft transplantation has been considered for the preservation of meniscal tissue. However, concerns over limited availability, disease transmission, immune rejection, and anatomical mismatching adversely influence its application⁴. In addition, although the initial mechanics are appropriate, dense tissue is not well suited for cellular infiltration and remodeling, resulting in poor and inconsistent long-term outcomes⁵. Hence, it is important to develop new strategies for meniscus transplantation.

To overcome these limitations, different kinds of tissue-engineered scaffolds have been developed^{6, 7}, including using biomaterials to fabricate porous scaffolds, seeding cells on the scaffold, and adding growth factors for cell proliferation and differentiation⁸. A functional, tissue-engineered scaffold should mimic the biomechanical structure of the meniscus and have appropriate mechanical properties to bear stress from different directions⁹. Traditional methods for scaffold fabrication, such as lyophilization, solvent casting, phase separation, and electrospinning, cannot meet these requirements¹⁰.

Three-dimensional (3D) printing can be used to manufacture objects with a desired size and structure and has been applied in meniscus scaffold fabrication for many years. The main steps of 3D printing meniscus scaffolds include the preparation of bioink, reconstruction of the 3D digital model of the meniscus, and 3D printing¹¹. Most studies have used MRI or CT scanning to obtain 3D digital models of a meniscus. Some researchers have used computer-aided design (CAD) to design a digital scaffold based on a 3D digital meniscus, then printed the scaffold and added other matrix and culture bioactive cells to the scaffold^{12, 13}. Some studies have printed a hollow scaffold with a relatively closed surface and added the matrix to the hollow scaffold¹⁴. Several studies have used bioink to directly print the meniscus based on a digital model^{15, 16}.

The microstructure of the meniscus is extremely complicated due to the complexity of the mechanical environment within the knee. Electron microscopy imaging studies have revealed three distinct layers of the collagen sheets in a meniscal cross-section: a superficial network that covers the surfaces by a meshwork of very thin fibrils (30 nm); a lamellar layer

beneath the superficial network, represented by a layer of lamellae of collagen fibrils (150–200 nm); and a central main portion, composed of predominantly circular-oriented bundles of collagen fibrils with occasional radial-tie fibers¹⁷. The mechanical properties are the most important features of these materials and are the first to be considered in regenerative medicine and tissue engineering¹⁸. Unfortunately, the scaffolds mentioned above barely mimic the microstructure of the meniscus and, therefore, do not obtain the same initial or long-term mechanical properties as an intact meniscus. One of the most important reasons is that these studies did not obtain a 3D printer readable microscale 3D digital model. Jeffrey *et al.*¹⁴ printed a meniscus 3D injection mold and injected a mix of cells, alginate, and CaSO₄ into the mold. After a few weeks of culture, the tissue was engineered. The construction can reach the highest equilibrium modulus at 60 kPa, which is 50% of native tissue. Several studies^{19–22} have used 3D printed PCL scaffold meniscal regeneration, which has a compressive modulus in the range of 10–54 MPa and a tensile modulus in the range of 40–80 MPa; the tensile modulus of these scaffolds is almost significantly lower than that of human menisci (78–125 MPa). These PCL scaffolds were designed by CAD according to a 3D digital meniscus model. It can be concluded that the mechanical properties of these scaffolds are far from those of native tissue. One of the most important reasons may be that the scaffold did not mimic the microstructure of the meniscus fibers. More specifically, the 3D microscale digital model is still lacking in resolution.

Therefore, it is urgent to develop a method to efficiently reconstruct a 3D-printer readable and microstructure mimicking meniscus model. The aim of this study is: (i) to explore the characteristics of meniscus microstructure; (ii) to reconstruct the meniscus microstructure; and (iii) to print a 3D model of the meniscus based on the digital model.

In this study, we used hematoxylin and eosin (HE) and Masson staining to analyze the histological features of the meniscus. Scanning electron microscopy (SEM) was used to help understand the meniscus microstructure. Menisci were acquired and scanned by high-resolution micro-MRI and micro-CT. We hypothesize that micro-MRI and micro-CT two-dimensional (2D) images can display the microstructure as the SEM does and that a microscale 3D digital model can be reconstructed based on the micro-MRI or micro-CT file.

Methods

All experimental protocols were approved by the Zhujiang Hospital of Southern Medical University Review Board. Informed consent was obtained from all subjects.

Specimen Preparation

Four menisci were removed from four TKA human knees (two men, two women; mean age, 56.5 ± 7.5 [standard deviation]) years without gross meniscal tears. One mature sheep meniscus was purchased from a butcher. The menisci were washed with phosphate-buffered saline (Sigma-Aldrich, St. Louis, MO, USA).

Histological Analysis

A human meniscus was fixed in 10% (v/v) buffered formalin, dehydrated with a series of graded alcohols, and embedded in paraffin. Tissue sections (4- μ m thick) were stained with HE²³ for morphologic analysis and Masson's trichrome²⁴ for cross-linked collagen.

Preparation of Freeze-Dried Menisci

The freeze-drying protocol was documented in our previous publication²⁵. Briefly, A human meniscus (4.7 cm \times 4.3 cm) was frozen at -60°C overnight and transferred to a freeze-drying machine (Alpha 2-4 LSCplus, Martin Christ Gefriertrocknungsanlagen, Germany), in which the water inside the frozen meniscus was sublimated under a pressure of 0.105 Pa and at a temperature of -40°C . The freeze-drying process lasted for 5 days.

Scanning Electron Microscopy

A small section of freeze-dried human meniscus was cut into thin slices. Samples were sputter-coated with gold prior to SEM observation. The samples were then imaged using SEM (JSM- 7600F, JEOL, Japan).

Micro-MRI Scanning

A human meniscus sample (4.7 cm \times 3.2 cm) was placed in the bottom of the scanning tube, and the tube was filled with distilled water. After sample preparation, the tube was placed into the head coil of the micro-MRI (M3; Aspect Imaging, Jerusalem, Israel) and scanned in the T2 phase. Each sample underwent continuous scanning with a scanning accuracy of 50 μ m (slice thickness, 1 mm; interslice gap, 0.1 mm; horizontal field of view, 12 mm; vertical field of view, 25 mm; pixel size, 0.05 mm). After scanning, the 2D images were exported as DICOM files²⁶.

Micro-CT scanning

The freeze-dried human meniscus was scanned in a μ CT 50 compact cabinet micro-CT scanner (SCANCO Medical AG, Bassersdorf, Zurich, Switzerland). The scanning settings were as follows: energy/intensity, 55 kVp, 109 μ A, 6 W; filter, 0.1 mm Al; calibration, 55 kVp, 0.1 mm Al; integration time, 1500 ms; average data, 3; FOV/diameter, 35.2 mm; voxel size, 11.4 μ m. The images were saved as DICOM (Digital Imaging and Communications in Medicine).

Three-Dimensional Printing

A sheep meniscus sample (2.7 cm \times 2.0 cm) was freeze-dried and scanned by micro-CT as described above. MATLAB 2015a (The MathWorks, Natick, MA) was used on a computer with an i7-4790K CPU and 16.0 GB memory to analyze the images. A 3D voxel model was reconstructed from the data, converted to STL format, and printed by resin with an enlarged size because of the limited accuracy of the 3D printer²⁵.

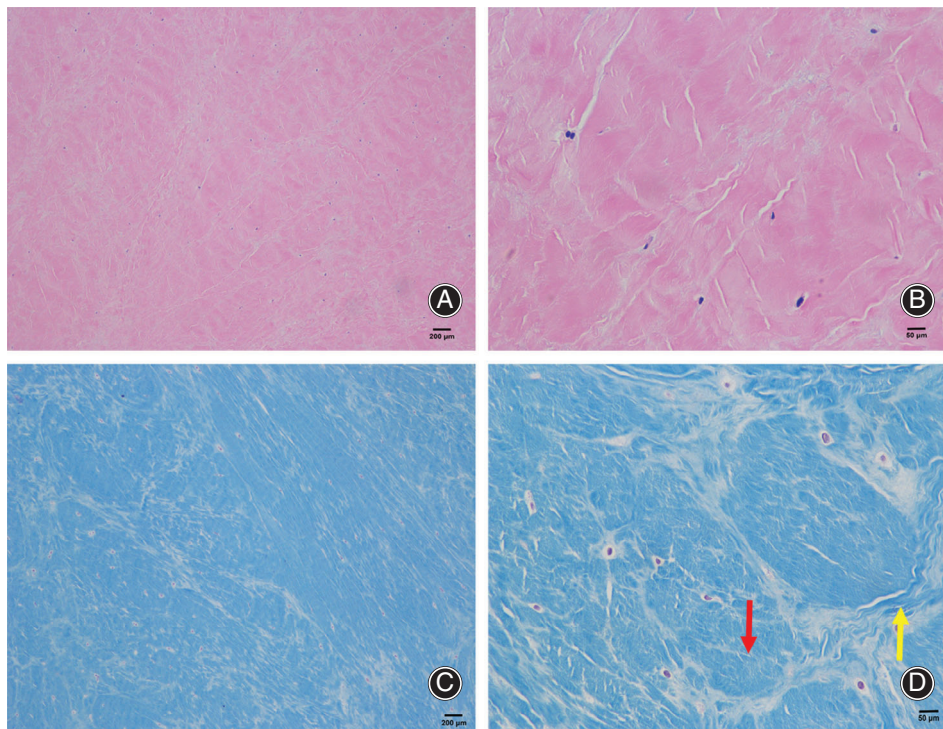


Fig. 1 Hematoxylin-eosin (HE) and Masson staining of the meniscus. A freshly harvested human meniscus was submitted to histological analysis by using HE and Masson staining. Histological analyses showed that the meniscus was mostly composed of collagen, with a few cells disseminated in the collagen. Masson staining displayed aligned collagen fiber bundles (yellow arrow, D) and circumferential fibers (red arrow, D). A and B are HE staining. C and D are Masson staining.

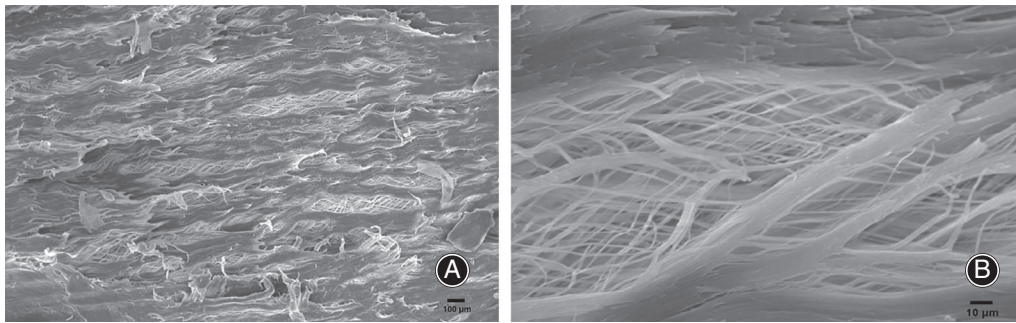


Fig. 2 Scanning electron microscopy (SEM) images of freeze-dried meniscus. A freeze-dried human meniscus was submitted to SEM. (A) In the SEM images, massive aligned fibers are clearly visible. At a higher level of magnification (B), varied diameters of fibers can be distinguished, and the fibers are highly cross-linked with numerous pores. The porosity of the meniscus according to SEM images was 34.1% ($34.1\% \pm 0.032\%$).

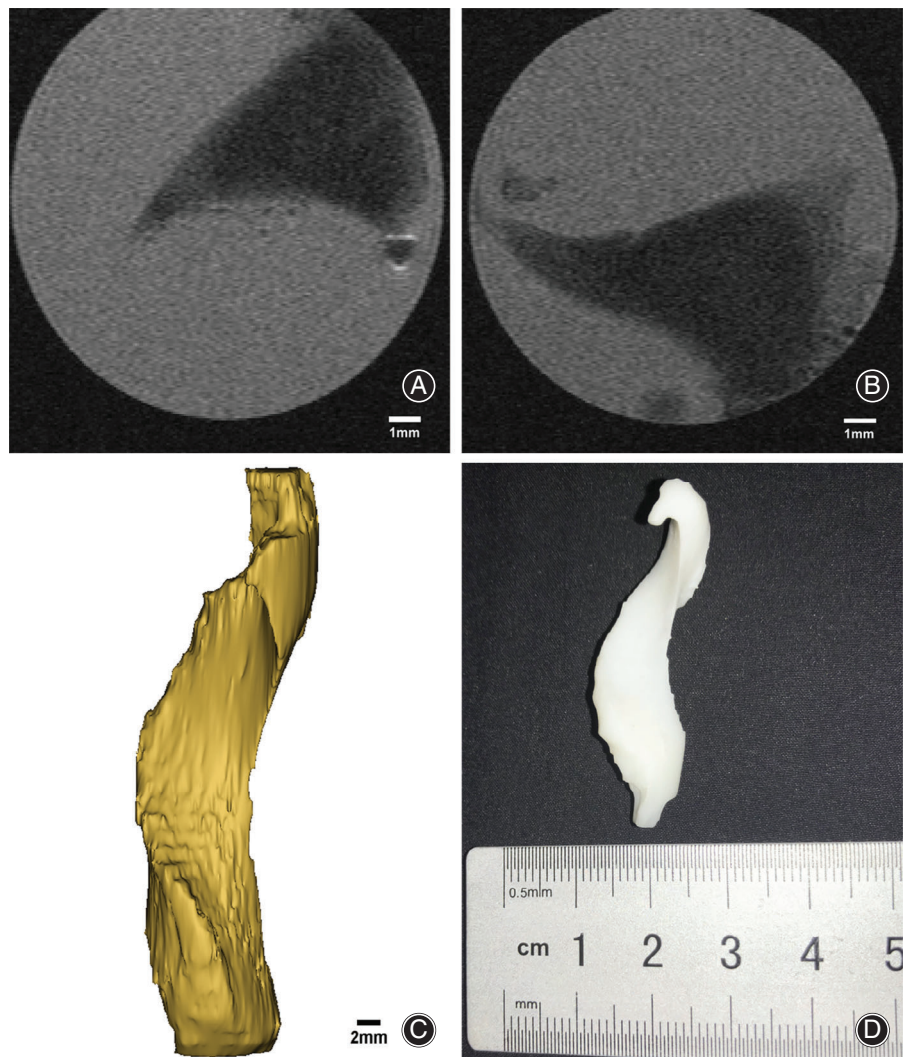


Fig. 3 Micro-MRI based three-dimensional (3D) reconstruction. A freshly harvested meniscus was immersed in distilled water and scanned by micro-MRI with a resolution of 50 μm . The outline of the meniscus is clear in micro-MRI two-dimensional images, but the microstructure is obscure (A, B). A voxel model of the meniscus was reconstructed (C). A resin 3D model was printed based on the voxel model (D).

Porosity Measurement

Porosity is defined as the ratio of the volume of pores to the volume of bulk rock and is usually expressed as a percentage.

Porosity gives biomaterials the ability to allow tissue infiltration and integration. It is usually the main factor taken into account during the design and synthesis of a biomaterial. SEM

images and micro-CT images of the meniscus were submitted to porosity measurement using Image J (version 1.47 for Windows, 64 bit, free software, National Institutes of Health, Bethesda, MD, USA). Briefly, the images were opened with image J. After thresholding was done, the porosity was determined by using the image volume method to sum up porosity pixels of all analyzed images and by dividing that value by the sum of the areas observed on these images. Then this obtained value was multiplied by 100%.

Results

Histological Characteristics

Hematoxylin–eosin staining and Masson staining showed that the meniscus was mostly composed of collagen, with a few cells disseminated between the collagen bundles (Fig. 1). Moreover, Masson staining revealed aligned collagen fiber bundles and circumferential fibers (Fig. 1D).

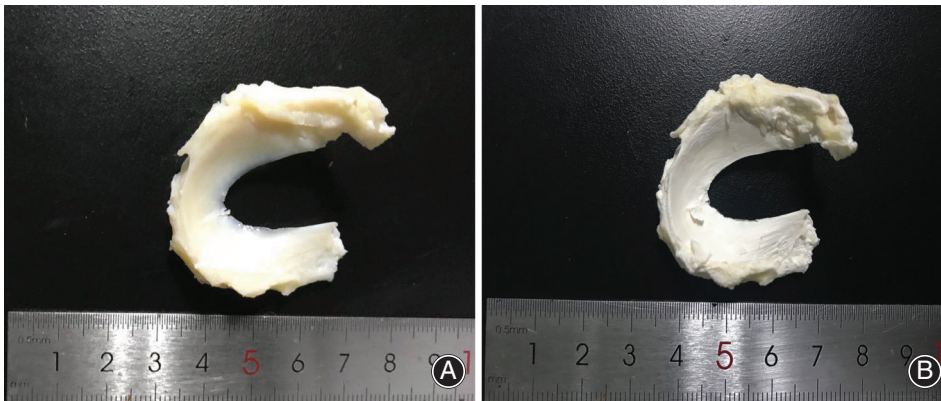


Fig. 4 Freeze-drying of a human meniscus. The shape of the freshly harvested human meniscus was freeze-dried. The fresh human meniscus (A) and freeze-dried meniscus (B) are almost the same.

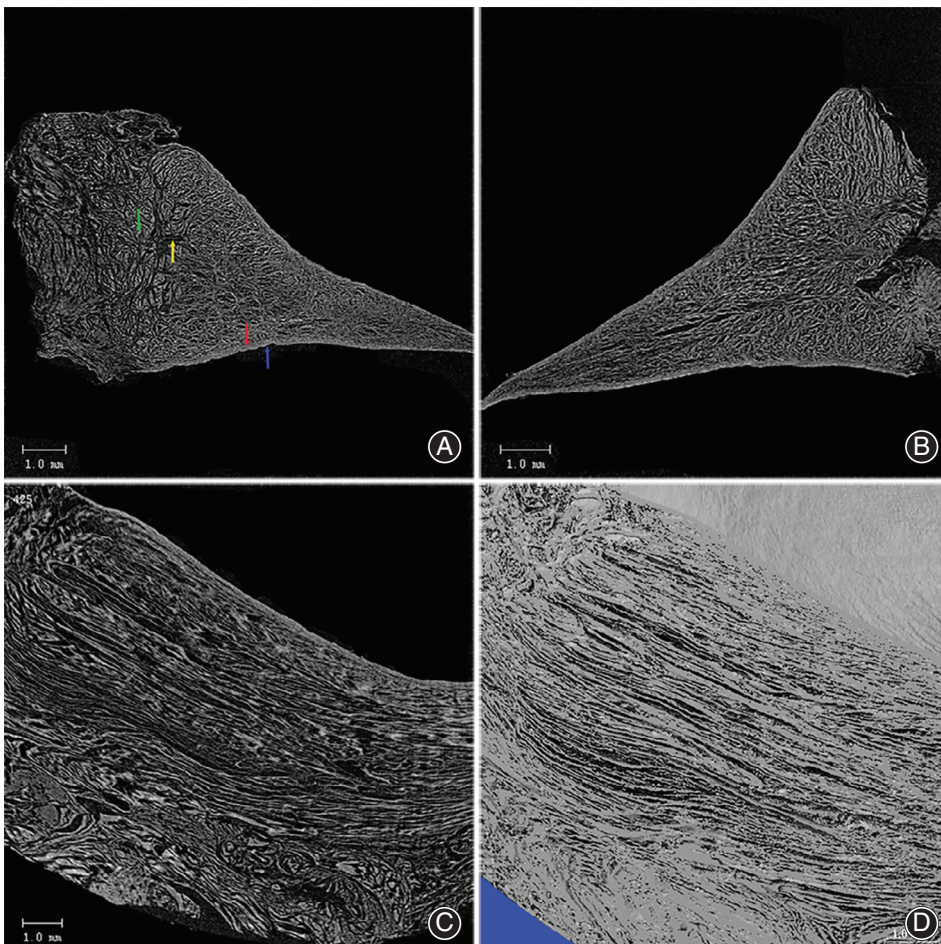


Fig. 5 Micro-CT scanning of freeze-dried meniscus. The freeze-dried meniscus was scanned by the micro-CT with a resolution of 11.4 μm . From the sagittal section of the micro-CT images (A, B), we can distinguish the surface layer (blue arrow, A), lamellar layer (red arrow, A), circumferential fibers (green arrow, A), and radial fibers (yellow arrow, A). (B) The sagittal section of another portion of the same meniscus. (C) The transverse section of meniscus micro-CT images. (D) The transverse section of the reconstructed model clearly displayed the route of a single fiber. The mean porosity of the meniscus according to micro-CT images was 33.92% (33.92% \pm 0.03%).

Scanning Electron Microscopy Analysis

In SEM images, massive aligned fibers are present (Fig. 2A). At a higher level of magnification (Fig. 2B), varied diameters of fibers can be found, and the fibers are highly cross-linked with numerous pores. The diameters of the collagen fibers are varied and the cross-linking pattern of the fibers is irregular. The porosity of the meniscus according to SEM images was 34.1% ($34.1\% \pm 0.032\%$).

Micro-MRI-Based Reconstruction

The outline of the meniscus is clear in micro-MRI images. Because of the limited diameter of the scanning container, the model seems to be twisted. The microstructure is obscure (Fig. 3A, B). Figure 3C displays a voxel model of the meniscus. A resin 3D model was printed based on the voxel model (Fig. 3D).

Micro-CT-Based Reconstruction

Figure 4A and B show a human meniscus before and after freeze-drying, respectively. The freeze-dried sample was subjected to micro-CT scanning. In the sagittal section of the micro-CT images (Fig. 5A), the surface layer (blue arrow), lamellar layer (red arrow), circumferential fibers (green arrow), and radial fibers (yellow arrow) are distinct. Figure 5B showed the sagittal section of another portion of the same meniscus. The path of the collagen fibers was clearly displayed in the transverse section (Fig. 5C). Even in the reconstructed digital model, the collagen fibers were distinct in the transverse section (Fig. 5D). The mean porosity of the meniscus according to micro-CT images was 33.92% ($33.92\% \pm 0.03\%$).

A 3D digital model of a sheep meniscus was reconstructed from the micro-CT files, and based on this digital model, an enlarged resin 3D meniscus model was printed (Fig. 6).

Discussion

Three-dimensional printed meniscus grafts are an emerging and promising innovation for meniscus

transplantation. However, current 3D-printed meniscus grafts are barely mechanically functional, primarily because these grafts poorly mimic the original microstructure of a meniscus. In this study, a histological method and SEM were used to analyze the characteristics of the meniscus microstructure. The highly cross-linked fibers and massive micropores indicate the difficulty in reconstructing the complicated microstructure of the meniscus. Micro-MRI and micro-CT were used to scan the meniscus. Compared to micro-MRI, the freeze-drying and micro-CT strategy is better in displaying the microstructure and reconstructing the printer-readable meniscus digital model.

Microstructure Analysis of the Meniscus

Of all the functions of the meniscus, load bearing and stabilizing are the most important. Under normal circumstances, the meniscus suffers from compressive and shear forces from different flexion angles. To withstand these forces, the meniscus has a unique structure and composition.

Specifically, the meniscus is composed of water, cells, and extracellular matrix. The extracellular matrix includes collagen, proteoglycans, and adhesion glycoproteins²⁷. As is evident from the HE and Masson staining, a few cells are disseminated between a large number of fibers.

According to SEM, the fibrous structure of the meniscus can be divided into three layers. The superficial layer, which contacts the tibial and femoral surface, is composed of a meshwork of thin fibrils. Beneath the superficial layer is the lamellar layer, which is a layer of lamellae of collagen fibrils on the tibial and femoral surfaces. The central layer, which is the main portion of the meniscus collagen fibrils, is located in the central region between the femoral and tibial surface layers. It contains radially aligned collagen fiber bundles and circumferential fibers.

The lamellar, circumferential, and radial fibers form a complex network within the meniscus that helps it to withstand the varied forces (e.g. shear, tension, and compression) to which it is exposed. The lamellar layer is known to serve as an envelope for the circumferentially-oriented fiber bundles in

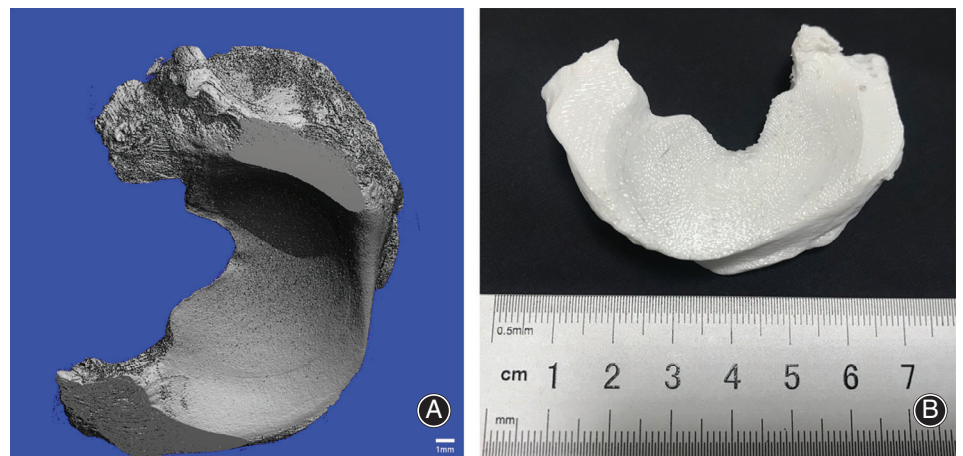


Fig. 6 Micro-CT-based three-dimensional (3D) reconstruction. A sheep meniscus was harvested and freeze-dried and scanned by micro-CT. A 3D voxel model of a sheep meniscus was reconstructed based on the micro-CT images (A). A 3D resin model of a sheep meniscus was printed out based on the digital model (B).

the central main portion of the meniscus and is well suited to facilitate surface-to-surface motion. Choi *et al.* found that the normal lamellar layer plays a considerable role in the resistance to a compressive load, especially at the contact surfaces between the articular cartilage and meniscus²⁸. The large and thick C-shaped bending fibers help resist tension and transfer the knee joint load for the meniscus. Moreover, radially scattered fibers (e.g., the “rope”), which strengthen the meniscus, prevent longitudinal tears caused by excessive pressure. Overall, the extremely complicated microstructure of the meniscus ensures its intricate mechanical function. In the SEM image of our study, we can see that the diameter of the fibers is varied. In addition, fibers are highly cross-linked, and between the fibers are numerous pores, which are suitable for cell migration. Considering the complicated fiber structure and the crosslinking of the fibers, it is almost impossible to fabricate a scaffold mimicking the meniscus using traditional methods. Therefore, 3D printing has become a promising approach to solve this problem. Theoretically, only if an original 3D printer readable digital model is obtained can any object be printed using the additive method of 3D printing.

Reconstruction and Three-Dimensional Printing of Meniscus Microstructure

To reconstruct the digital model, we used micro-MRI to scan the meniscus. The healthy meniscus tissue has a short T2 on MRI, which means these tissues exhibit low intensity on conventional MR images. In our study, the meniscus sample showed low intensity on MRI. The meniscus microstructure could not be discriminated on the MR image. However, the outline was obvious. A 3D digital model was reconstructed based on the MR images, and a resin 3D meniscus model was printed. Because the diameter of the container that holds the meniscus sample was limited, the sample was twisted in the container, resulting in a distorted 3D model. However, the shape was precise. Our result was comparable to published studies that used MR images to reconstruct the model^{19, 21}. Choi *et al.* used ultrashort echo time MR images to display the lamellar layer, which may be a future direction of meniscus MR imaging²⁸.

As a result, micro-CT was taken into consideration. However, soft tissue cannot be viewed clearly on micro-CT because it has a high water content²⁹. To improve the contrast of biological tissue in micro-CT imaging, many contrast agents have been used to label the target tissue and to image the microstructure

more clearly^{30–33}. Unfortunately, the resulting images and 3D microstructures of these digital models are insufficient to allow 3D printing. Researchers have used micro-CT to scan rough menisci. The outline can be reconstructed, but the microstructure is obscure^{14, 34}. Freeze-drying is a sublimation process that removes moisture from materials at low temperatures while maintaining their structure, bioactivity, and other properties. We freeze-dried the meniscus before micro-CT scanning. Surprisingly, the CT image not only showed a precise outline but also displayed a relatively clear microstructure of the meniscus. From the transverse CT image, the surface layer, lamella layer, circumferential fibers, and radial fibers could be identified. Moreover, a resin 3D model was printed based on the micro-CT files, which clarified that this microscale 3D digital model was printable. Chen *et al.*³⁵ (2018) used 3D micro-printing to fabricate freestanding polymer 3D nanostructures. Combined with our study, we believe that a biomimic micro-printed meniscus is achievable in the near future.

Limitations

Our study has some limitations. First, limited by the resolution of the micro-CT we used, the exact path of the inner fibers was not as clear as in the SEM images. Second, few 3D printer and printing materials could match the nano-scale printing accuracy, which limited the precision of the 3D model of the meniscus. In addition, the regional variation of the fiber path was not fully analyzed in this study. The present study was the first attempt to reconstruct the microstructure of a meniscus using a freeze-drying and micro-CT strategy. In future study, we will reconstruct more accurate models and analyze the microstructure more systematically.

Conclusion

The most important findings of our study are that a lyophilized meniscus can be scanned by micro-CT, the micro-CT image clearly displays the microstructure of the meniscus, and a reconstructed microscale 3D digital model is printable. This study provides a new strategy to reconstruct the microstructure of the meniscus, providing a crucial step towards the completely biomimicked 3D printing of the meniscus.

ACKNOWLEDGMENTS

This work was supported by the National Natural Science Foundation of China (grant no. 81801210).

References

- Makris EA, Hadidi P, Athanasiou KA. The knee meniscus: structure-function, pathophysiology, current repair techniques, and prospects for regeneration. *Biomaterials*, 2011, 32: 7411–7431.
- Lin Z, Huang W, Ma L, *et al.* Kinematic features in patients with lateral discoid meniscus injury during walking. *Sci Rep-Uk*, 2018, 8: 5053.
- Heijink A, Gomoll AH, Madry H, *et al.* Biomechanical considerations in the pathogenesis of osteoarthritis of the knee. *Knee Surg Sports Traumatol Arthrosc*, 2012, 20: 423–435.
- Shimomura K, Hamamoto S, Hart DA, Yoshikawa H, Nakamura N. Meniscal repair and regeneration: current strategies and future perspectives. *J Clin Orthop Trauma*, 2018, 9: 247–253.
- Noyes FR, Barber-Westin SD. Long-term survivorship and function of meniscus transplantation. *Am J Sports Med*, 2016, 44: 2330–2338.
- Bilgen B, Jayasuriya CT, Owens BD. Current concepts in meniscus tissue engineering and repair. *Adv Healthc Mater*, 2018, 7: e1701407.
- Chen M, Guo W, Gao S, *et al.* Biochemical stimulus-based strategies for meniscus tissue engineering and regeneration. *Biomed Res Int*, 2018, 2018: 8472309.
- Monibi FA, Cook JL. Tissue-derived extracellular matrix bioscaffolds: emerging applications in cartilage and meniscus repair. *Tissue Eng Part B Rev*, 2017, 23: 386–398.
- McNulty AL, Guilak F. Mechanobiology of the meniscus. *J Biomech*, 2015, 48: 1469–1478.
- Cucchiari M, McNulty AL, Mauck RL, Setton LA, Guilak F, Madry H. Advances in combining gene therapy with cell and tissue engineering-based approaches to enhance healing of the meniscus. *Osteoarthritis Cartilage*, 2016, 24: 1330–1339.

11. Shen S, Chen M, Guo W, *et al.* Three dimensional printing-based strategies for functional cartilage regeneration. *Tissue Eng Part B Rev*, 2019, 25: 187–201.
12. Buyuksungur S, Tanir TE, Buyuksungur A, *et al.* 3D printed poly (ϵ -caprolactone) scaffolds modified with hydroxyapatite and poly (propylene fumarate) and their effects on the healing of rabbit femur defects. *Biomater Sci-Uk*, 2017, 5: 2144–2158.
13. Filardo G, Petretta M, Cavallo C, *et al.* Patient-specific meniscus prototype based on 3D bioprinting of human cell-laden scaffold. *Bone Joint Res*, 2019, 8: 101–106.
14. Balllyns JJ, Gleghorn JP, Niebrzydowski V, *et al.* Image-guided tissue engineering of anatomically shaped implants via MRI and micro-CT using injection molding. *Tissue Eng Part A*, 2008, 14: 1195–1202.
15. Borges RA, Choudhury D, Zou M. 3D printed PCU/UHMWPE polymeric blend for artificial knee meniscus. *Tribol Int*, 2018, 122: 1–7.
16. Wei J, Wang J, Su S, *et al.* 3D printing of an extremely tough hydrogel. *RSC Adv*, 2015, 5: 81324–81329.
17. Andrews SHJ, Rattner JB, Abusara Z, Adesida A, Shrive NG, Ronsky JL. Tie-fibre structure and organization in the knee menisci. *J Anat*, 2014, 224: 531–537.
18. Pina S, Ribeiro VP, Marques CF, *et al.* Scaffolding strategies for tissue engineering and regenerative medicine applications. *Materials*, 2019, 12: 1824.
19. Cengiz IF, Pitikakis M, Cesario L, *et al.* Building the basis for patient-specific meniscal scaffolds: from human knee MRI to fabrication of 3D printed scaffolds. *Bioprinting*, 2016, 1: 1–10.
20. Szojka A, Lalh K, Andrews SH, Jomha NM, Osswald M, Adesida AB. Biomimetic 3D printed scaffolds for meniscus tissue engineering. *Bioprinting*, 2017, 8: 1–7.
21. Zhang Z, Wang S, Zhang J, *et al.* 3D-printed poly (ϵ -caprolactone) scaffold augmented with mesenchymal stem cells for total meniscal substitution: a 12-and 24-week animal study in a rabbit model. *Am J Sports Med*, 2017, 45: 1497–1511.
22. Bahcecioğlu G, Hasirci N, Bilgen B, Hasirci V. A 3D printed PCL/hydrogel construct with zone-specific biochemical composition mimicking that of the meniscus. *Biofabrication*, 2019, 11: 025002.
23. Fischer AH, Jacobson KA, Rose J, Zeller R. Hematoxylin and eosin staining of tissue and cell sections. *CSH Protoc*, 2008, 2008: t4986.
24. Ouyang J, Guzman M, Desoto-Lapaix F, Pincus MR, Wieczorek R. Utility of desmin and a Masson's trichrome method to detect early acute myocardial infarction in autopsy tissues. *Int J Clin Exp Pathol*, 2009, 3: 98–105.
25. Zhu S, Zhu Q, Liu X, *et al.* Three-dimensional reconstruction of the microstructure of human acellular nerve allograft. *Sci Rep*, 2016, 6: 30694.
26. Yao Z, Yan LW, Wang T, *et al.* A rapid micro-magnetic resonance imaging scanning for three-dimensional reconstruction of peripheral nerve fascicles. *Neural Regen Res*, 2018, 13: 1953–1960.
27. Fox AJS, Bedi A, Rodeo SA. The basic science of human knee menisci: structure, composition, and function. *Sports Health*, 2012, 4: 340–351.
28. Choi J, Biswas R, Bae WC, *et al.* Thickness of the meniscal lamellar layer: correlation with indentation stiffness and comparison of normal and abnormally thick layers by using multiparametric ultrashort echo time MR imaging. *Radiology*, 2016, 280: 161–168.
29. Wang Y, Ma J, Yin T, *et al.* Correlation between reduction quality of femoral neck fracture and femoral head necrosis based on biomechanics. *Orthop Surg*, 2019, 11: 318–324.
30. Nelson J, Huang X, Steinbrener J, *et al.* High-resolution x-ray diffraction microscopy of specifically labeled yeast cells. *Proc Natl Acad Sci U S A*, 2010, 107: 7235–7239.
31. Gignac PM, Kley NJ. Iodine-enhanced micro-CT imaging: methodological refinements for the study of the soft-tissue anatomy of post-embryonic vertebrates. *J Exp Zool B Mol Dev Evol*, 2014, 322: 166–176.
32. Descamps E, Sochacka A, De Kegel B, Van Loo D, Van Hoorebeke L, Adriaens D. Soft tissue discrimination with contrast agents using micro-CT scanning. *Beig J Zool*, 2014, 144: 20–24.
33. Qiu X, Cheng L, Wang B, *et al.* Micro perfusion and quantitative analysis of the femoral head intraosseous artery. *Orthop Surg*, 2018, 10: 69–74.
34. Deng C, Yao Q, Feng C, *et al.* 3D printing of bilineage constructive biomaterials for bone and cartilage regeneration. *Adv Funct Mater*, 2017, 27: 1703117.
35. Chen M, Xu Z, Kim JH, Seol SK, Kim JT. Meniscus-on-demand parallel 3D Nanoprinting. *ACS Nano*, 2018, 12: 4172–4177.